JMEPEG (1998) 7:163-172

Recent Advances in the Hole Drilling Method for Residual Stress Measurement

M. Beghini and L. Bertini

(Submitted 15 August 1997; in revised form 8 September 1997)

The main activities in the hole drilling residual stress measurement technique recently developed at the University of Pisa are reviewed and presented. Particular attention was paid to developing tools for increasing the limits indicated by the presently applied standard procedures for residual stress evaluation. For residual stresses that were assumed to be uniform through-thickness, the effect of plasticity was numerically analyzed and results formed the basis for a procedure that allows an increase in the maximum measurable residual stress up to 0.9 of the material yield strength. For nonuniform through-thickness residual stress, accurate analytical influence functions are proposed by which arbitrary interpolation of the influence coefficients is avoided and all the experimentally obtained strains, with no regard to their number, can be used as input for residual stress evaluation.

Keywords hole drilling, residual stress, plasticity, through-thickness variability

1. Introduction

The hole drilling method (HDM) is a semidestructive experimental technique for measuring residual stress (RS) at the surface of a body. It is based on the measurement of the strain produced by the local stress relaxation induced by drilling a small-diameter hole (typically 1 to 5 mm). A complete evaluation of the relaxed strain field (in the elastic regime) can be obtained by a three-gage rosette, whose typical shape is shown in Fig. 1.

In the standard procedure, as defined for instance by ASTM E 837-95 (Ref 1), the complete RS field (i.e., principal stress values and orientation) can be evaluated from the strains measured by the rosette, by means of relationships based on the elastic plane stress solution for an infinite body having a pass-through hole and subjected to uniform through-thickness stress at infinity.

Such a procedure has two main drawbacks, which can significantly restrict the practical applicability of the HDM. The first is related to the hypothesis of linear elastic material behavior. Indeed, in order to limit the effect of plasticity on the measurement, the maximum measurable RS is set to one-half of the material yield strength. The second limitation is connected with the requirement of through-thickness RS uniformity. Significant variations of RS with depth are often observed in practical applications.

Due to the high practical importance of the HDM, a relevant amount of research has been devoted to overcome these limitations, particularly the second one. Mainly collecting partial results recently published by the authors, this paper gives a general overview of the work carried out at the University of Pisa in these fields. It is a part of a wider research activity that includes theoretical and experimental studies on the influence of RS on fracture and fatigue crack growth of materials and structures (Ref 2, 3).

Regarding the effects of plasticity, a procedure is proposed that allows a satisfactory evaluation of RS up to 90% of material yield strength. Regarding the through-thickness RS variability, the aim is the development of analytical influence functions, that can make RS evaluation more simple and accurate.

The present contribution is mainly of a methodological nature and is intended to propose more accurate and general tools for elaborating measured strains in order to obtain residual stresses. As for any other experimental procedure, some aspects of these methodologies require direct validation. This is particularly true for the effect of plasticity. These experimental activities are now under development and no conclusive result has been yet reached.

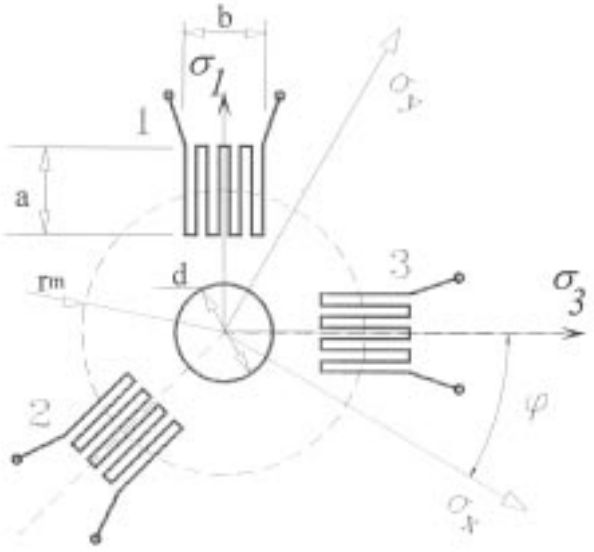

Fig. 1 Typical standard rosette for hole drilling residual stress measurement

M. Beghini and **L. Bertini,** Dipartimento di Costruzioni Meccaniche e Nucleari, via Diotisalvi, No. 2 56126 Pisa, Italy.

2. Residual Stress Evaluation with Plasticity

2.1 Problem Formulation and Discussion of Analytical Approaches

Even though RS is elastic, the HDM can produce local plasticity near the hole boundary due to the notch effect. This increases the strain actually measured as compared to an elastic material, producing an overestimate of the RS. In these conditions the equations usually employed to relate residual stresses to measured relaxed strains are obviously no longer valid. In the following a procedure applicable to elastic-plastic conditions is described.

Following the same approach employed in deriving linear elastic relationships suggested by ASTM, the study was conducted with reference to the following (ideal) cases:

- Infinite plate, in plane stress conditions, carrying a pass-through hole (PTH)
- Semi-infinite body carrying a blind hole (BH)

For both cases, a uniform stress distribution was assumed at large distance from the hole and the material was considered to exhibit a bilinear stress-strain behavior. This required two more material properties: the yield strength, σ_{ys}, and the tangent modulus (defined for uniaxial loading) in plastic regime, E_p.

The infinitely extended body hypothesis is currently employed in the standard HDM procedure, even in the absence of plastic phenomena, and therefore its use does not imply significant loss of generality. It is, however, the responsibility of the analyst to decide about the applicability of this hypothesis in particular cases, providing for alternative analysis methods (e.g., deriving specific correlation functions by numerical analyzes or calibration techniques) whenever validity is questionable (e.g., for measures in the neighborhood of sharp notches or edges).

As regards the hypothesis of a bilinear stress-strain law, it must be observed that in HDM, strains produced by stress relaxation are relatively small (within 1% for typical metallic materials). As a consequence, the material plastic behavior can be linearly approximated without significant errors, provided that this relationship is specifically selected in order to reproduce the near-yield stress-strain curve. It is well known that the results of an elastic-plastic analysis can be strongly affected by the choice of the yielding point and that several definitions, mainly of a conventional nature, are usually adopted for this point, particularly for a material having a smooth stress-strain curve. In our opinion, the possibility of choosing different strain hardening coefficients can reduce the arbitrariness of this choice because two parameters are available to fit the local stress-strain behavior. However, a proper analysis is necessary for correctly setting these parameters. A study on this aspect, also involving experimental verifications, is now under development.

A general solution for the two reference cases cannot be reached by completely analytical methods. Particular solutions were obtained for the PTH problem under equibiaxial loading and assuming an elastic/perfectly plastic material (Ref 4, 5). An analytical solution for the same problem in the presence of general biaxial loading conditions is proposed in (Ref 6) under the questionable hypothesis of a plastic zone completely surrounding the hole. This hypothesis was not confirmed by numerical analyzes (Ref 7), and moreover, this approach does not appear to be suitable for practical applications due to the complexity of the expressions relating RS and relaxed strains and to the lack of an account for the influence of material strain hardening properties, which are often significant near yielding. No analytical solution is available for the BH problem.

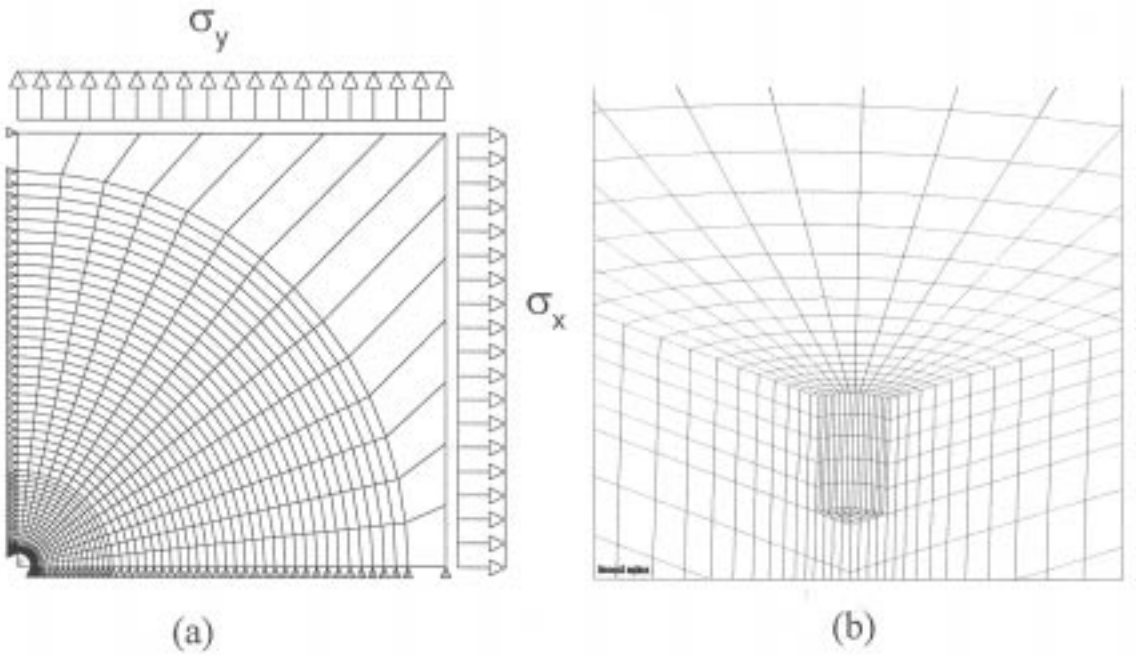

Fig. 2 FE models for elastic-plastic analyses. (a) Plane stress model for PTH. (b) 3-D model for BH

2.2 Finite Element Analyses

Due to these difficulties, it became necessary to solve the proposed problems by means of a numerical method. The finite element (FE) models reported in Fig. 2(a) and (b) were set up, making use of the ANSYS FE code, in order to analyze the PTH and the BH problems, respectively. The presence of a general biaxial residual stress field was simulated by imposing uniform pressure distributions on the sides not containing the hole. These pressures were assumed to be equal to the principal residual stresses in the body before the hole was drilled.

The overall dimensions of these models and the size and distribution of elements were defined, through a preliminary convergence analysis, to ensure the independence of results (within less than 0.5%) from mesh parameters. An in-plane model size equal to 30 times the hole radius was selected for both cases, and the model thickness was set to 5 times the maximum hole depth for the BH.

The accuracy of results was further checked by comparison with available analytical solutions. For pure elastic analysis, the relationships given in (Ref 1) were assumed as reference for both models, while in the elastic-plastic regime the comparison was possible only for PTH using the results from Ref 5 (elastic/perfectly plastic material and axysymmetric loading). In any case, differences less than 1% were observed, which were considered satisfactory for the present purpose.

The strain gage response was evaluated by averaging strain on the strain gage active grid region. The influence of the following parameters was taken into account:

- Residual stress intensity
- Biaxiality ratio: $\Omega = \sigma_x/\sigma_y$ (Eq 1)
- Hardening coefficient: $r = E_p/E$ (Eq 2)
- Rosette orientation : φ

Geometrical symmetries and the hypothesis of equal tensile and compressive material behavior allowed us to limit the range of analysis for the biaxiality ratio between –1 (pure shear) to 1 (equibiaxial). Five Ω values were examined in this range (–1, –0.414, 0, 0.414, 1). As regards to the RS intensity, nine loading levels were selected for each biaxiality ratio, ranging from the onset of plasticity at the hole boundary to near-complete body yielding. A representation of the analyzed loading conditions is reported in Fig. 3. The initial yielding locus, determined for PTH by the elastic theoretical solution, was also employed to define the lower-level loading conditions for the BH problem.

Four hardening coefficients were considered: 0.01 (used for numerically reproducing perfectly plastic material), 0.1,

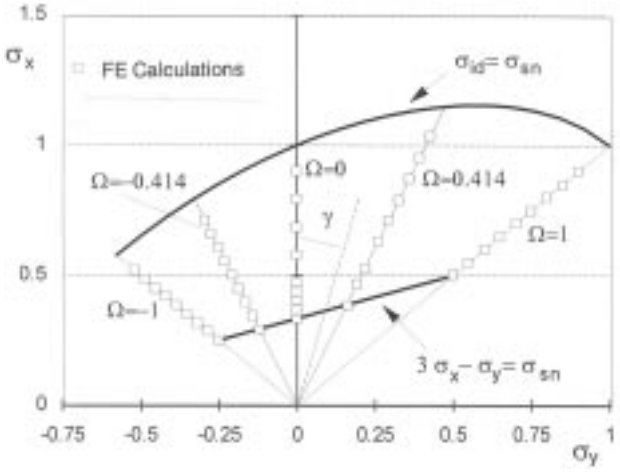

Fig. 3 Loading conditions for the elastic-plastic calculations

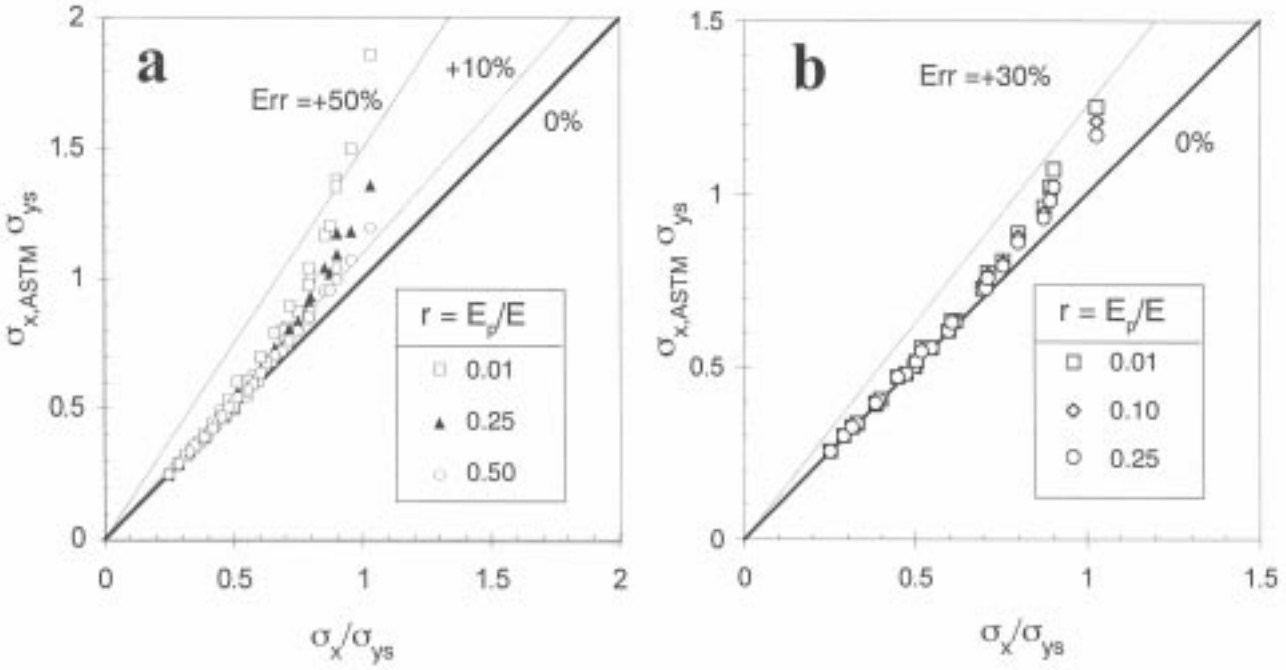

Fig. 4 Errors due to the direct application of the ASTM standard during RS measurements for different material properties. (a) PTH. (b) BH

0.25, and 0.5. These values were thought to adequately represent the near-yielding strain hardening properties of actual materials. In the end 360 elastic-plastic FE analyzes were performed.

2.3 Main Results and Discussion

For each FE analysis, the readings of an ASTM standard rosette were calculated at several angular orientations around the hole. These numerically simulated strains were then applied as input data in the standard ASTM procedure (valid for elastic material only). The so-obtained stress components, hereafter called $\sigma_{i,ASTM}$ ($i = x, y$), were employed to directly evaluate the errors produced by neglecting plasticity.

The calculated maximum principal stress for all the load cases is reported in Fig. 4 as a function of the actual value for PTH and BH. It can be observed that, neglecting plasticity, residual stresses may be overestimated by more than 60 to 70% and 30%, respectively, under unfavorable conditions. Because these errors appear unacceptable for many practical applications, a general-purpose procedure capable of giving a more accurate RS prediction in the presence of plastic strain was developed on the basis of these results.

With the focus on obtaining a comparable representation of the RS level for any biaxiality ratio, a dimensionless factor f representing loading intensity was defined as:

$$f = \frac{\sigma_{eq} - \sigma_{eq,i}}{\sigma_{ys} - \sigma_{eq,i}} \qquad \text{(Eq 3)}$$

where $\sigma_{eq,i}$ is the equivalent (Mises) RS producing the onset of yielding (see Fig. 2). The loading factor f is negative when the material is elastic and assumes values ranging between 0 (onset of yielding) and 1 (general plate yielding) in the plastic regime for any biaxiality ratio.

In Fig. 5 the ratio between the readings of two strain gages aligned with RS principal directions, $\bar{\varepsilon}_y$ and $\bar{\varepsilon}_x$, is plotted as a function of the loading factor. This ratio seems to be nearly independent of the loading level. This observation suggested that the biaxiality ratio can be estimated from the ratio between the strains measured in the principal directions, by using the following relationship, valid in the elastic regime:

$$\Omega = \frac{\sigma_y}{\sigma_x} \cong \frac{(A - B) - \dfrac{\bar{\varepsilon}_y}{\bar{\varepsilon}_x}(A + B)}{\dfrac{\bar{\varepsilon}_y}{\bar{\varepsilon}_x}(A - B) - (A + B)} \qquad \text{(Eq 4)}$$

where A and B are coefficients given by ASTM (Ref 1) depending on the material elastic constants and on the rosette and hole geometry. The nearly equal sign in Eq 4 indicates that this equation is approximately valid in the elastic-plastic regime too. This allows us to estimate Ω in the elastic-plastic regime by the measured strains in the principal directions $\bar{\varepsilon}_x$ and $\bar{\varepsilon}_y$.

The effective loading factor f is compared to f_{ASTM} in Fig. 6 for the PTH case (similar trends were observed for the BH case). The relationship between the two quantities appears to be well represented by a parabolic law, whose coefficient C is a function of the biaxiality ratio:

$$f_{ASTM} = f + C(\Omega)f^2 \qquad \text{(Eq 5)}$$

A suitable expression for C was obtained by a fitting technique, giving:

$$C = 0.793(1 - r)^{2.167}[0.6495 \sin(2\gamma) + 1] \text{ for the PTH} \qquad \text{(Eq 6a)}$$

$$C = (0.167 - 0.281r)[\sin(2\gamma) + 0.299 - 0.390r] \text{ for the BH} \qquad \text{(Eq 6b)}$$

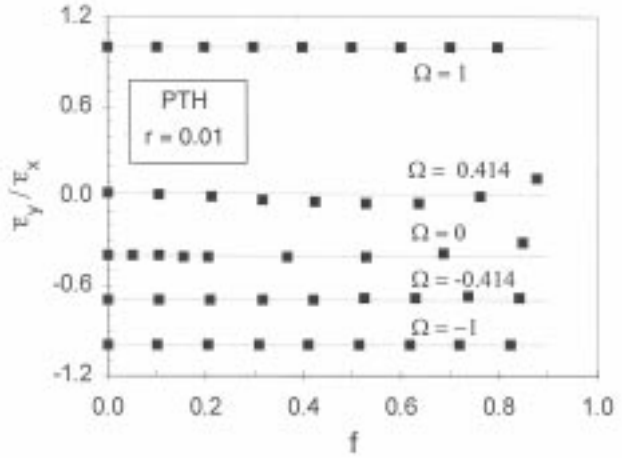

Fig. 5 Ratio between strain measured in the principal directions vs. loading intensity for several biaxiality ratios. In the figure a particular case is shown, but similar trends were observed for other strain hardening cases and also for BH.

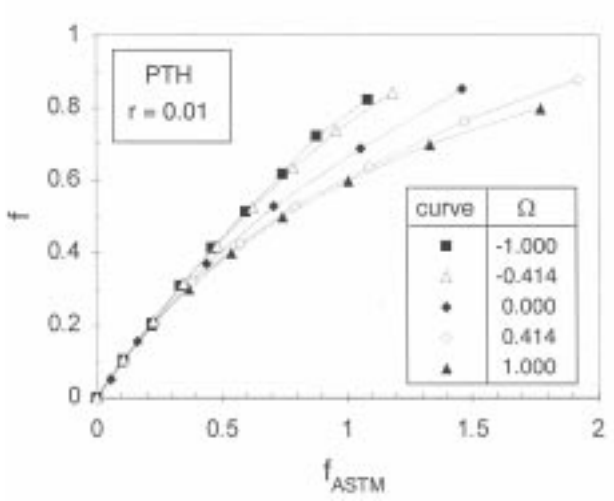

Fig. 6 Effective vs. ASTM estimated loading factors. Both numerically estimated points (symbols) and fitting curves (Eq 5) are shown.

where $\gamma = \tan^{-1}\Omega$ (biaxiality angle).

An estimate of the effective loading factor can be obtained by solving Eq 5:

$$f_{es} = \frac{\sqrt{1 + 4Cf_{ASTM} - 1}}{2C} \quad \text{(Eq 7)}$$

Once the equivalent residual stress and the biaxiality ratio are known, the principal residual stress values $\sigma_{x,es}$ and $\sigma_{y,es}$ can be estimated as:

$$\sigma_{x,es} = \sigma_{ys}\left[f_{es}\cdot\left(\frac{1}{\sqrt{\Omega^2 - \Omega + 1}} - \frac{1}{3-\Omega}\right) + \frac{1}{3-\Omega}\right] \quad \text{(Eq 8a)}$$

$$\sigma_{y,es} = \Omega\sigma_{x,es} \quad \text{(Eq 8b)}$$

where Ω is given by Eq 4.

The comparison of the maximum residual stress obtained by Eq 8(a) and (b) with actual values for all the analyzed cases is reported in Fig. 7. The error is usually less than $0.02\sigma_{ys}$, reaching $0.05\sigma_{ys}$ in the worst condition ($r = 0.01$, $\sigma_{eq} = 0.9\sigma_{ys}$, PTH). The error on the minimum principal stress was found to be less than $0.10\sigma_{ys}$.

If the principal directions are not known, the angle φ and the extreme strain values $\bar{\varepsilon}_x$ and $\bar{\varepsilon}_y$ must be evaluated from the readings of the three strain gages: $\bar{\varepsilon}_1$, $\bar{\varepsilon}_2$, and $\bar{\varepsilon}_3$. This induces a new source of error. Indeed, when plasticity is negligible, the measured strain exhibits a sinusoidal dependence from the strain gage angular position and the three measurements of the rosette give the necessary and sufficient conditions for evaluating the required extreme values $\bar{\varepsilon}_x$ and $\bar{\varepsilon}_y$, and the angle φ. Unfortunately, in the elastic-plastic regime, the angular dependence of measured strain is no more sinusoidal, and in general, the extreme values cannot be evaluated only on the basis of the three readings obtainable from a standard rosette generically oriented. If a sinusoidal approximation of the effective angular dependence is applied, the accuracy of the results is affected by the rosette orientation.

Figure 8 shows the maximum RS calculated with Eq 8(a) and by applying the sinusoidal approximation for determining $\bar{\varepsilon}_y/\bar{\varepsilon}_x$ for different orientations of the rosette (φ = 0°, 15°, 30°, and 45°, PTH case). As a consequence of the error in the evaluation of the extreme strain values, results in Fig. 8 are affected by a scatter higher than in Fig. 7(a) (material properties and loading conditions are the same).

For many practical purposes the obtainable precision is still acceptable (compare to Fig. 4), the errors on the maximum residual stress component being not greater than 20% in the worst condition ($r = 0.01$). However, an improvement can only be reached when the principal directions are known and the rosette is placed so that $\varphi = 0$. In this case strain gages 1 and 3 in Fig. 1 directly give the required strains.

2.4 *Procedure for Residual Stress Measurement above $0.5\sigma_{ys}$*

Based on the above considerations, the following general procedure can be applied in order to reduce the error in estimating high residual stresses:

1. Compute the principal RS ($\sigma_{x,ASTM}$, $\sigma_{y,ASTM}$) and the angle of the x principal direction with the rosette (φ) by the standard ASTM procedure (i.e., assuming a linear elastic material behavior).

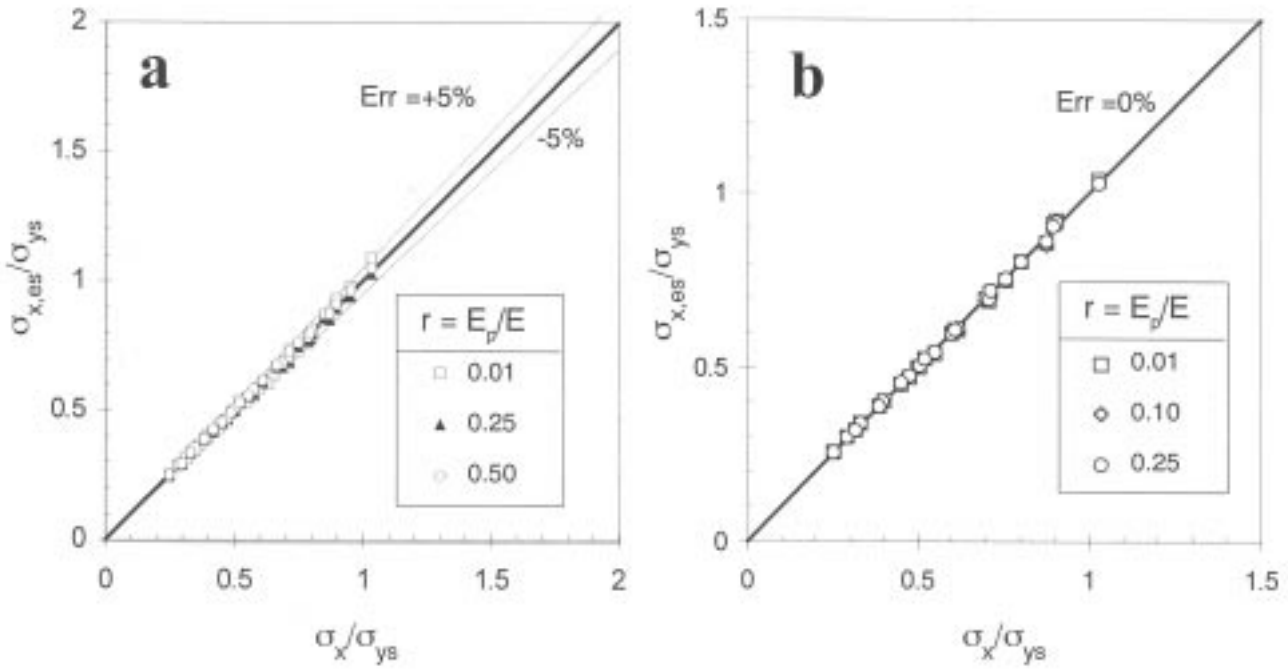

Fig. 7 Comparison between true maximum RS and that estimated by the proposed procedure (Eq 8a, b) when the strains in the principal directions are known. (a) PTH. (b) BH

2. Compute the biaxiality factor value (Ω). To this end, two situations are to be considered:

- Residual stress principal directions are known. Gages 1 and 3 have to be aligned with the principal directions, so that they directly measure the extreme strain values $\bar{\varepsilon}_x$ and $\bar{\varepsilon}_y$. The biaxiality factor can then be calculated as:

$$\Omega = \frac{(A-B) - \frac{\bar{\varepsilon}_y}{\bar{\varepsilon}_x}(A+B)}{\frac{\bar{\varepsilon}_y}{\bar{\varepsilon}_x}(A-B) - (A+B)} \quad \text{(Eq 9)}$$

- Principal directions are unknown. In this case the biaxiality factor must be approximated by:

$$\Omega = \frac{\sigma_{y,\mathrm{ASTM}}}{\sigma_{x,\mathrm{ASTM}}} \quad \text{(Eq 10)}$$

3. Compute $\sigma_{eq,i}$ and the elastic load intensity factor:

$$\sigma_{eq,i} = \sigma_{ys}\frac{\sqrt{(1-\Omega+\Omega^2)}}{(3-\Omega)} \quad \text{(Eq 11)}$$

$$f_{\mathrm{ASTM}} = \frac{\sigma_{eq,\mathrm{ASTM}} - \sigma_{eq,i}}{\sigma_{ys} - \sigma_{eq,i}} \quad \text{(Eq 12)}$$

4. Compute the estimated load parameter, f_{es} by Eq 7.
5. Compute the stress level by Eq 8.

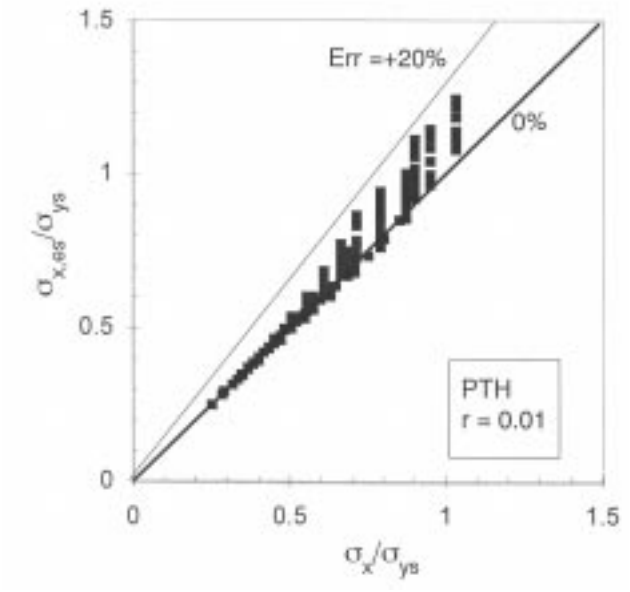

Fig. 8 Maximum RS estimated on the basis of a standard three-gage rosette variously oriented (0°, 15°, 30°, 45°) by assuming a sinusoidal angular dependence for strain

2.5 Proposal for an Alternative Measurement Method

As shown, the accuracy of results is in general reduced by the distortion of the angular dependence of the strain due to plasticity. This effect cannot be eliminated without further data. When principal directions are unknown a modified rosette is proposed.

It has been noted that the actual strain angular dependence can be described satisfactorily by adding one further term in the Fourier expansion, i.e., assuming the following relationship for the measured strain:

$$\bar{\varepsilon} = C_0 + C_1\cos(2(\varphi+\chi)) + C_2\cos(4(\varphi+\chi)) \quad \text{(Eq 13)}$$

that includes the elastic solution as a particular case ($C_2 = 0$).

The evaluation of the unknown parameters (φ, C_0, C_1, C_2) of Eq 13 requires four independent conditions. For this reason the use of a four-gage rosette, as shown in Fig. 9, is proposed, whose readings $\bar{\varepsilon}_1$, $\bar{\varepsilon}_2$, $\bar{\varepsilon}_3$, and $\bar{\varepsilon}_4$ give the necessary and sufficient conditions to evaluate the unknown coefficients in Eq 13.

By this rosette a sufficiently accurate prediction of the extreme strains $\bar{\varepsilon}_x$ and $\bar{\varepsilon}_y$ can be obtained in spite of the rosette orientation. Figure 10 shows the results of using this rosette for evaluating the extreme strain values in the cases of Fig. 8. The trend and the scatter are both comparable to those of Fig. 7, which are the best obtainable with the proposed method and can be accepted in many practical situations.

3. Analytical Influence Functions for Variable Residual Stress Analysis

3.1 Variable Residual Stress

In many cases when RS evaluation is of interest (e.g., after surface treatments), the dependence of RS on depth cannot be

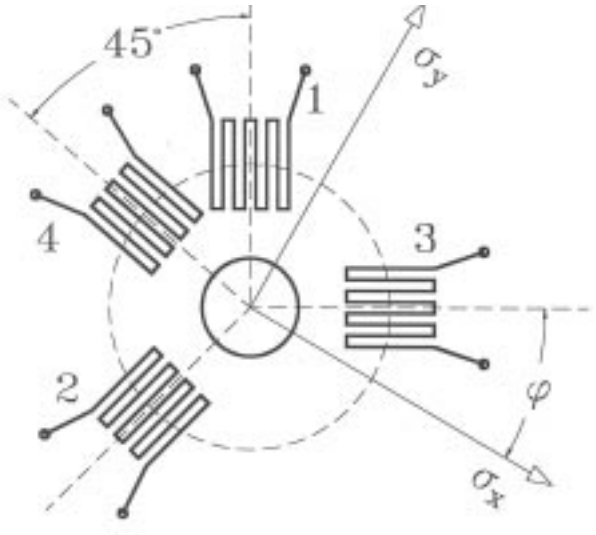

Fig. 9 Proposed four-gage rosette for high residual stress measurement

neglected. Information about the through-thickness variation of RS can be obtained by drilling holes in a sequence of steps and recording the strain gage readings at any step. This amount of data has to be elaborated for having the RS distribution along the hole depth.

A valuable contribution to the development of a correct procedure for obtaining through-thickness RS distribution was done by Schajer (Ref 8, 9) on the basis of a FE parametric analysis. Schajer's approach is based on numerically evaluated influence coefficients by which a system of linear equations can be written relating RS distribution in the *Z* direction to the relaxed strains obtained at several hole depths (*z*) (see Fig. 11). Hereafter, capital letters indicate Cartesian coordinates and lower case *z* indicates hole depths.

Schajer discussed two methods for evaluating variable residual stresses: the integral method and the power series method. In the former, which is the more widely employed, the domain of analysis (ranging from zero to the final hole depth) is divided into a finite number of intervals and RS is approximated by a discontinuous stepping function, constant within each interval.

The influence coefficients are given only for a finite number of regularly spaced hole depths and positions along the hole surface. However, it is common that experimental hole depths differ from those numerically simulated, thus requiring two-dimensional interpolation.

In the following, a proposal is presented for replacing the discrete influence coefficients with continuous functions, called influence functions.

3.2 Problem Statement

In accordance with ASTM E 835-95 and referring to Fig. 1 and 11, the following assumptions were made:

- Linear elastic homogenous isotropic material
- Plane stress condition for local RS field (i.e., σ_{xx}, σ_{xy}, σ_{yy} >> σ_{xz}, σ_{yz}, σ_{zz}) with components independent to *X* and *Y* (in the zone of the hole) and variable only with *Z*
- Semi-infinite solid, i.e., hole diameter (*d*) negligible as compared to any significant linear dimension of the body

As shown by Schajer, under these hypotheses the problem can be simplified by adopting the following scalar stress components (which are functions of *Z* only):

$$P(Z) = (\sigma_3 + \sigma_1)/2$$
$$Q(Z) = (\sigma_3 - \sigma_1)/2$$
$$T(Z) = \sigma_{13} \quad \text{(Eq 14)}$$

where σ_1, σ_3, and σ_{13} indicate normal and shear stress components in the reference system aligned with the rosette (Fig. 1). Similarly, the following quantities of the measured strain (which are functions of the hole depth *z* only) can be defined:

$$p(z) = (\bar{\varepsilon}_3 + \bar{\varepsilon}_1)/2$$
$$q(z) = (\bar{\varepsilon}_3 - \bar{\varepsilon}_1)/2$$
$$t(z) = (\bar{\varepsilon}_3 - \bar{\varepsilon}_1 - 2\bar{\varepsilon}_2)/2 \quad \text{(Eq 15)}$$

where $\bar{\varepsilon}_1$, $\bar{\varepsilon}_2$, and $\bar{\varepsilon}_3$ are the strain gage measurements during drilling and therefore functions of *z*. Quantities *P* and *p* are related to the equibiaxial residual stress-strain level, while *Q* , *T* and *q*, *t* are related to the stress-strain shear level. It can be demonstrated that, using these quantities, the following equalities hold:

$$p(z) = \int_0^z I_A \cdot P(Z)dZ$$
$$q(z) = \int_0^z I_B \cdot Q(Z)dZ$$
$$t(z) = \int_0^z I_B \cdot T(Z)dT \quad \text{(Eq 16)}$$

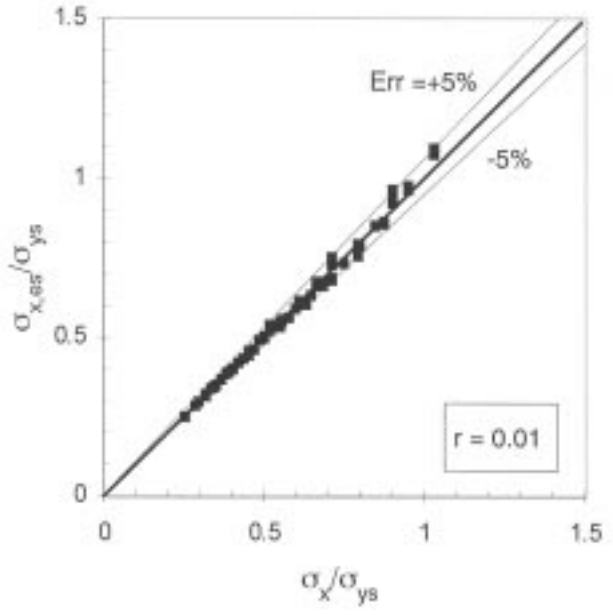

Fig. 10 Evaluation of maximum RS by a variously oriented four-gage rosette (0°, 15°, 30°, 45°)

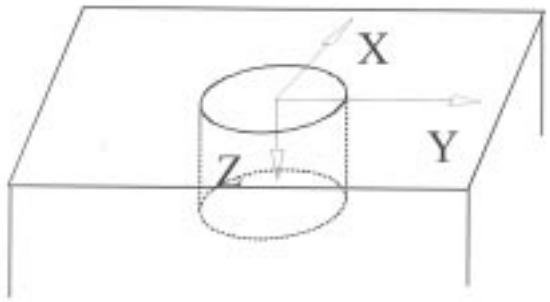

Fig. 11 Scheme for the through-thickness variable RS evaluation

where I_A and I_B are suitable influence functions of geometry and material properties to be determined.

If the influence functions I_A and I_B were available, Eq 16 could be regarded as three integral equations in which p, q, and t are known while P, Q, and T are unknown functions. In practical applications, p, q, and t functions are obtained by strain measurements while influence functions must be evaluated by theoretical or numerical methods.

3.3 Influence Function Analysis

Under the hypotheses indicated in the previous section, the following general expression can be written for the influence functions (I_A is used as an example):

$$I_A = I_A(a, b, r_m, d, E, \nu, z, Z) \quad \text{(Eq 17)}$$

in which three kinds of quantities can be distinguished:

- Geometrical parameters, mainly related to experimental arrangement
- Material properties
- Geometrical variables

In order to obtain an approximate expression, some simplifications can be introduced in Eq 17. First, from the results of the general theory of elasticity, the dependence of E can be made explicit because any component of strain is inversely proportional to the Young's modulus for a given external loading and geometry. Moreover, geometrical parameters can be reduced by adopting dimensionless quantities. As usual in this kind of problem, the mean radius of the rosette (r_m) was taken as the reference distance, and consequently the following dimensionless geometrical quantities were defined:

$$\begin{aligned} \phi &= d/r_m \\ \xi &= a/r_m \\ \eta &= b/r_m \\ h &= z/r_m \\ H &= Z/r_m \end{aligned} \quad \text{(Eq 18)}$$

Moreover, by assuming a particular rosette (or any other geometrically self-similar), ξ and η can be fixed and the general expressions for the influence functions can be further simplified as follows:

$$\begin{aligned} I_A &= \frac{1}{E} \cdot A(\varphi, \nu, h, H) \\ I_B &= \frac{1}{E} \cdot B(\varphi, \nu, h, H) \end{aligned} \quad \text{(Eq 19)}$$

in which the independent variables cannot be further reduced without lacking generality.

3.4 FE Analysis

An approximate analytical expression for the influence functions was obtained on the basis of a series of linear elastic FE analyzes. A virtually semi-infinite body was modeled by means of plane Fourier isoparametric 8-node elements. This allowed the simulation of both the equibiaxial and pure shear loading required to obtain information related to I_A and I_B. Figure 12 illustrates the FE model, which includes zones having different element densities (total number of degrees of freedom was approximately 7200). Strain gage measurements were obtained as described in the previous section. A preliminary convergence study was conducted to assess the accuracy of results. The estimate accuracy in strain evaluation was about 1%.

In order to reduce the number of required FE analyzes, a reference condition was considered by fixing the following typical parameters: $\nu = 0.3$ and $\phi = 0.8$. This required two further influence functions to be defined:

$$\begin{aligned} A_0(h, H) &= E \cdot I_A(0.8, 0.3, h, H) \\ B_0(h, H) &= E \cdot I_B(0.8, 0.3, h, H) \end{aligned} \quad \text{(Eq 20)}$$

A sequence of 40 hole depths were analyzed by means of an automatic procedure in which successive element layers were removed. For any hole depth h a sequence of loading conditions were analyzed by assuming a unitary uniform pressure applied from $H = 0$ to $H = H^*$ where $H^* \leq h$ for any of them. The corresponding values of the strain on the rosette were calculated. With these results, a set of integral conditions of the following type can be written:

$$\int_0^{H^*} A_0(h, H)\, dH = E \cdot p_n(h, H^*) \quad \text{(Eq 21)}$$

where $p_n(h, H^*)$ is the calculated equibiaxial strain component.

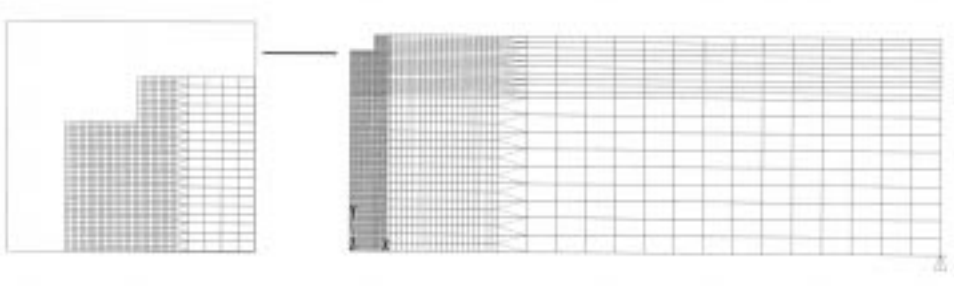

Fig. 12 FE model for evaluation of influence functions. Details of the hole region are shown.

Equation 21 may be regarded as a set of conditions that the unknown function $A_0(h, H)$ has to satisfy. A double series expansion was assumed for it:

$$A_0(h, H) = \sum_{i=1}^{n} \sum_{j=1}^{n} \alpha_{ij} H^{n-i} h^{n-J} \qquad \text{(Eq 22)}$$

in which α_{ij} are coefficients to be evaluated.

By substituting Eq 22 into Eq 21, the integral equation is transformed into a linear algebraic equation having α_{ij} as unknowns. The number of these equations is limited only by the number of FE analyzes to be performed and by the element through-thickness spacing. In the present case about 820 numerically simulated strain measurements were used for each influence function.

It was observed that $n = 6$ (36 unknown quantities) offered a reasonable compromise between accuracy and numerical stability. The number of unknowns was considerably smaller than the number of equations and a least-squares solution was adopted for solving the linear system.

In Fig. 13 the integral value of the calculated function is plotted, and the function itself is reported in Fig. 14. By assuming $n = 6$ the analytically defined surface in Fig. 13 is in fairly good agreement with the FE obtained values (the two solutions are not distinguishable in that scale and the FE solution is not reported for clarity). An estimate of the accuracy of this influence function as regards to the FE evaluation can be obtained by introducing the following function:

$$\mathrm{err}_A(h, H*) = \frac{E \cdot p_n(h, H*) - \int_0^{H*} \sum_{i=1}^{6} \sum_{j=1}^{6} \alpha_{ij} H^{6-i} h^{6-J} dH}{E \cdot p_n(h, H*)} \qquad \text{(Eq 23)}$$

which measures the relative error in the solution of integral Eq 21. A plot of the error function is given in Fig. 15. It can be observed that the maximum difference is about 1% while the error is usually less than 0.5%. Because this accuracy is similar to that estimated for the FE analysis, no further increase in the number of unknowns was required.

A similar procedure was applied to the shear influence function, thus obtaining:

$$B_0(h, H) = \sum_{i=1}^{n} \sum_{j=1}^{n} \beta_{ij} H^{n-i} h^{n-J} \qquad \text{(Eq 24)}$$

which showed an accuracy similar to that of Eq 22 for $n = 6$. The calculated α_{ij} and β_{ij} coefficients are reported in Tables 1 and 2, respectively.

3.5 Discussion

By means of Eq 22 and 24 any influence coefficient can be obtained by a simple integration of polynomials. The matrices proposed by Schajer were thus calculated by using the obtained influence functions. Small differences (a few percent) were ob-

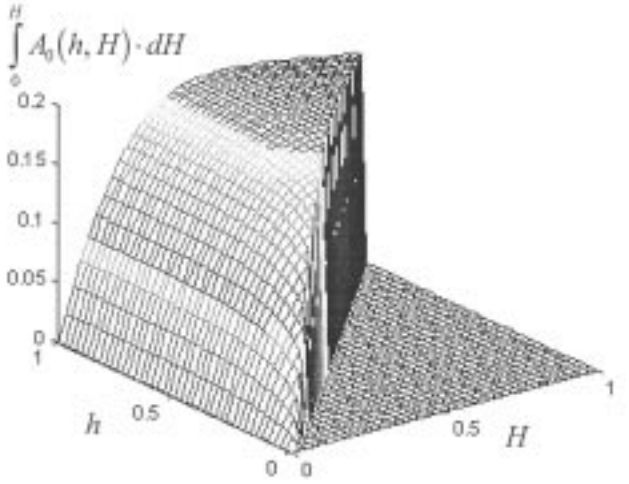

Fig. 13 Integral value for the reduced influence function A_0

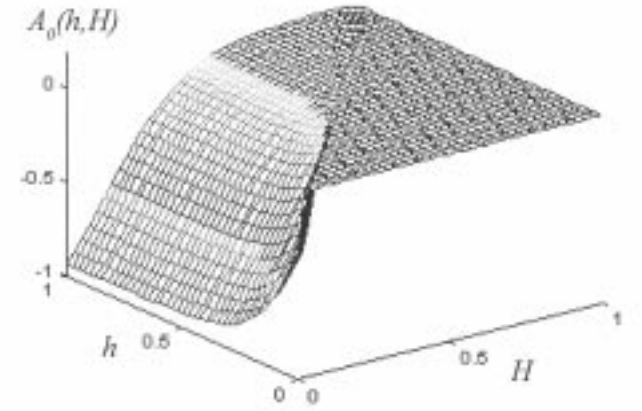

Fig. 14 Values of the reduced influence function A_0

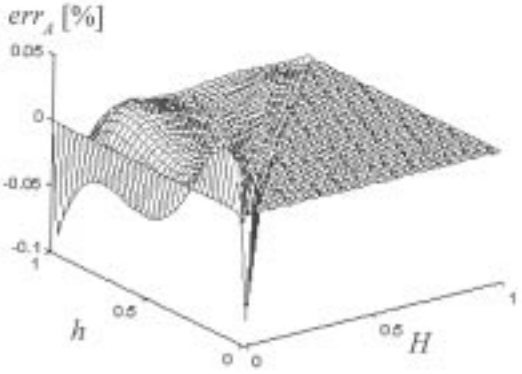

Fig. 15 Relative error on integrated A_0

Table 1 α_{ij} coefficients

i/j	1	2	3	4	5	6
1	7.94499E+02	–2.00261E+03	7.73108E+02	4.50399E+01	–2.34443E+01	–4.43709E+00
2	–1.75336E+03	7.10597E+03	–3.40893E+03	1.06428E+02	6.45780E+01	1.52406E+01
3	–3.87482E+02	–8.57291E+03	5.29455E+03	–5.12397E+02	–5.79213E+01	–2.10575E+01
4	3.69954E+03	3.29977E+03	–3.38436E+03	5.29955E+02	1.72611E+01	1.47916E+01
5	–3.15948E+03	6.40194E+02	6.99597E+02	–1.86427E+02	2.37442E-01	–5.37103E+00
6	7.93066E+02	–4.35446E+02	–5.36670E+00	2.57122E+01	1.84857E+00	–3.86883E-01

Table 2 β_{ij} coefficients

i/j	1	2	3	4	5	6
1	1.75992E+03	–3.30567E+03	1.13504E+03	1.92158E+02	–8.67759E+01	–2.54740E+00
2	–5.42858E+03	1.22611E+04	–5.33646E+03	–9.21497E+01	2.38296E+02	1.03604E+01
3	5.11779E+03	–1.62645E+04	8.64168E+03	–6.27958E+02	–2.33575E+02	–1.68976E+01
4	–5.08022E+02	8.85358E+03	–5.94844E+03	8.18798E+02	9.82501E+01	1.38004E+01
5	–1.39383E+03	–1.46253E+03	1.64114E+03	–3.36688E+02	–1.67071E+01	–5.67623E+00
6	4.32671E+02	–2.74571E+01	–1.86003E+02	6.53095E+01	1.02752E+00	–5.72400E-01

served in the first coefficients (for shallow holes and forces near the surface). It is reasonable to assume that those differences are due to the increased accuracy in the FE analyzes and that they affect the evaluation of residual stresses only near the free surface of the body.

The availability of a continuous expression for the influence functions eliminates arbitrary interpolation when the influence coefficients are requested for applying the integral method. Moreover, there is virtually no limit to the number of experimentally obtained hole depths. This is particularly useful in practical applications, as recently proposed electronically controlled hole drilling devices allow production of depth increments as small as 0.01 mm.

The present influence functions can also be easily used to obtain other influence coefficients, such as those required for the application of the power series method. In principle, this could allow us to apply the power series method by including a virtually unlimited number of terms, thus extending its applicability to fields where the integral method is currently preferred.

4. Summary

This paper has presented the results recently obtained at the University of Pisa in the improvement of the hole drilling method. It was concerned with two main topics, the effects of plasticity and the analysis of through-thickness variable stress.

As regards the effects of plasticity, based on a large number of numerical simulations of measurements, rather simple empirical relationships were written, which allow one to estimate uniform residual stresses higher than one-half the material yield strength. The rather large range of examined conditions ensures that the proposed relationships cover most of the situations that can be encountered in practical applications.

If the RS principal directions are known, the proposed procedure permits measurement of residual stresses up to 90% of the material yield strength, with errors contained within a few percent. For high stress values, the accuracy obtainable by using a standard three-gage rosette is affected by the rosette orientation and errors up to 20% can be expected. A notable improvement (errors within 5%) can be achieved by the introduction of a four-gage rosette that produces results practically independent of its orientation.

In the field of through-thickness variable RS evaluation, only linear elastic material response was examined. Analytical expressions for the influence functions have been proposed, which were obtained by numerical solution of integral equations, based on the results of accurate FE analyzes. These influence functions appear to give some advantages in variable RS analysis, compared to currently employed methods.

As regards future research activities, integration of the two approaches may be indicated, aimed at defining a procedure capable of analyzing variable RS fields in the elastic-plastic regime.

References

1. "Standard Test Method for Determining Residual Stress by the Hole-Drilling Strain-Gage Method," ASTM E 837-89, American Society for Testing and Materials, 1995
2. M. Beghini and L. Bertini, Fatigue Crack Propagation through Residual Stress Fields with Closure Phenomena, *Eng. Fract. Mech.*, Vol 36, 1990, p 379-387
3. M. Beghini, L. Bertini, and E. Vitale, Fatigue Crack Growth in Residual Stress Fields: Experimental Results and Modelling, *Fatigue Fract. Eng. Mater. Struct.*, Vol 17, 1994, p 1433-1444
4. M. Beghini, L. Bertini, and P. Raffaelli, An Account of Plasticity in the Hole-Drilling Method for Residual Stress Measurement, *J. Strain Anal.*, Vol 30, 1990, p 227-233
5. M. Beghini, L. Bertini, and P. Raffaelli, "Von Mises Criterion Elastic-Plastic Analysis of an Infinite Plate with a Hole," unpublished research, 1994
6. B.D. Annin and G.P. Cherepanov, *Elastic Plastic Problems*, ASME Press, New York, 1988
7. M. Beghini, L. Bertini, and P. Raffaelli, Numerical Analysis of Plasticity Effects in the Hole Drilling Residual Stress Measurement, *J. Test. Eval.*, Vol 22, 1994, p 522-529
8. G.S. Schajer, Application of Finite Element Calculations to Residual Stress Measurements, *J. Eng. Mater. Technol.*, Vol 103, 1981, p 157-163
9. G.S. Schajer, Measurement of Nonuniform Residual Stress Using the Hole Drilling Method, *J. Eng. Mater. Technol.*, Vol 110, 1988, p 338-349